

EXPLORING THE MAXIMUM SUPERHEATING MAGNETIC FIELDS OF NIOBIUM*

N. Valles[†], Z. Conway, M. Liepe, Cornell University, CLASSE, Ithaca, NY 14853, USA

Abstract

The RF superheating magnetic field of superconducting niobium was measured with a 1.3 GHz re-entrant cavity at several points in the temperature range from 1.6 K to 4.2 K. Measurements were made with $< 200 \mu\text{s}$ high power pulses ($\sim 1.5 \text{ MW}$). Our test incorporated oscillating superleak transducers to determine the cavity quench locations and characterize changes or the migrations of the quench locations during processing. This study builds upon previous work in that it tests the same re-entrant cavity again, after machining exterior grooves to increase the cooling of the cavity. After machining grooves into the cavity, new measurements of the critical RF magnetic field find the field to be linearly increasing as a function of $(T/T_c)^2$ down to 1.6 K, and allow discrimination between two competing theories for the behaviour of the field, namely the Vortex Line Nucleation Model and the Ginzburg-Landau theory.

INTRODUCTION

Over the past 30 years accelerating gradients in Niobium superconducting cavities have increased from 5 MV/m to over 55 MV/m [1]. To determine the maximal achievable gradient, we must understand the fundamental limit, the critical RF magnetic field, H_c^{RF} . Determining the limiting magnetic field is the purpose of this work.

The critical field is postulated to be the same as the superheating field [2], the field level above which a superconductor undergoes a phase transition to the normal conducting state. Two theories explaining the temperature dependence of the superheating field have been suggested. The Vortex Line Nucleation Model (VLMN), predicts that the superheating field depends on temperature, T , according to

$$H_{sh}(T) = 1780.4 \text{ Oe} \left[1 - \left(\frac{T}{T_c} \right)^4 \right]. \quad (1)$$

where $\bar{T}_c = 9.014 \text{ K}$ is the reduced critical temperature of Niobium [4]. The Ginzburg-Landau Theory, valid near T_c , predicts that the superheating field has the form

$$H_{sh}(T) = 1.2 H_0 \left[1 - \left(\frac{T}{T_c} \right)^2 \right] \quad (2)$$

where $H_0 = 2000 \text{ Oe}$, and for Niobium, $T_c = 9.2 \text{ K}$ [9]. The VLMN fits results from a BCP cavity [3, 4], but disagrees with an EP cavity test [5]. This study seeks to determine which model is correct by performing measurements

* Work supported by grants from the National Science Foundation and the Alfred P. Sloan Foundation.

[†] nrw5@cornell.edu

06 Material studies

of a very high quality Niobium cavity over a low temperature range, where differences between the two predictions become apparent.

The superheating field decreases with increasing temperature, so to ensure that bath thermometer accurately reflects the RF surface temperature, short, high power pulses (HPP) were used to minimize heating and grooves were machined onto the outer cavity surface to enhance cooling. The superheating field can be differentiated from a defect caused quench because as the limiting field is surpassed, the high magnetic field region should make a global transition to the normal conducting state. The origin of the quench, and whether or not it is a global transition can be determined with the use of oscillating superleak transducers (OSTs) [6]. The experimental set-up is pictured in Fig. 1.

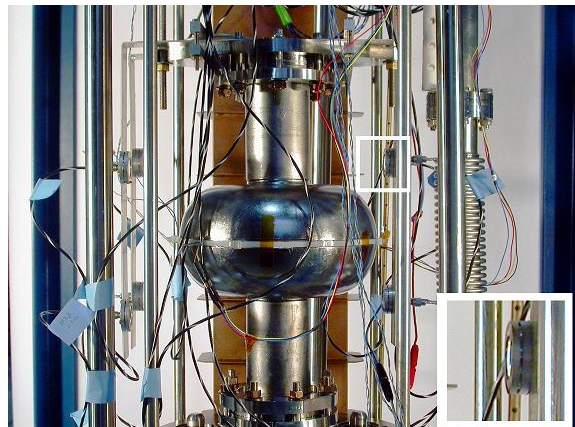


Figure 1: Experimental set-up showing 1.3 GHz re-entrant cavity mounted on a test stand. The copper waveguide behind the cavity connects to the klystron and supplies the HPP. Eight OSTs are mounted at corners of a cube around the cavity and are used to detect quench locations. An enlargement of an OST is shown in the lower right corner.

HEATING SIMULATIONS

To have confidence in the measurement of the superheating field as a function of temperature, the difference between the inner RF surface and the bath thermometer should be as small as possible. This experiment already implements short HPP, which rapidly excites the cavity without depositing a lot of RF energy, but to increase cooling, the effects of machining grooves on the outer surface of the cavity were investigated.

The high magnetic field region of this cavity extends about 1.5 cm on either side of the equator weld. This re-

gion was modelled using ANSYS, and the heating caused by the magnetic field during pulsed cavity operation was simulated, ramping the energy stored in the cavity from 0 to 35 J, corresponding to a maximum surface field of 1900 Oe, over 200 μ s. These values were chosen because they were the conditions used during the last experiment with this cavity [5]. The BCS resistance of the cavity is given by $R_s = R_0 + R_{BCS}(T)$, where R_0 , the residual resistance was taken to be 20 n Ω , and the BCS resistance is given by

$$R_{BCS}(T) = \frac{A}{T} \left(\frac{f}{f_0} \right)^2 \exp \left(-\frac{T_0}{T} \right) \quad (3)$$

with parameters $A = 2 \times 10^{-4} \Omega \cdot K$, $f_0 = 1.5$ GHz and $T_0 = 17.67$ K, where T is the temperature of the metal and f is the frequency of the RF wave, and is accurate for $T < T_c/2$ [2]. The simulation does not take into account high field Q slope; if it did, the temperature change at the end of a pulse would increase. This means that the simulations performed, set a lower bound on the temperature change during pulsed operation.

A simulation of this region with cooling grooves was also performed at temperatures in the 2.0–4.2 K range, and a heating simulation starting at 2.0 K is presented in Fig. 2.

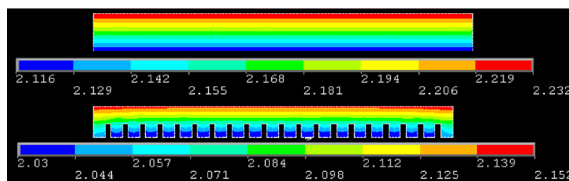


Figure 2: Comparison of temperature change of inner surface for grooved and ungrooved cavity initially at 2 K ramping up from 0 to 35 joules of energy stored in the cavity over 200 μ s.

Comparing the temperature change of the inner surfaces in the ungrooved case $\Delta T_{ungrooved}$ and the grooved case $\Delta T_{grooved}$, one finds the figure of merit at 2 K:

$$\frac{\Delta T_{ungrooved} - \Delta T_{grooved}}{\Delta T_{ungrooved}} = 30\%. \quad (4)$$

Thus, grooving the cavity reduces the temperature change during pulsed operation. The typical ΔT to be expected is approximately 0.2 K.

Another simulation was performed to compare the behaviour of the grooved cavity under uniform heating, and heating due to a line defect around the equator. ANSYS simulated the temperature increase of the cavity as the energy in the cavity was ramped up from 0 to 35 J over 200 μ s. In the first case, energy was dissipated through the entire high magnetic field. In the second case the same amount of energy was dissipated at a defect having a width of 100 μ m at the equator. The result is shown in Fig. 3.

This simulation suggests that for a localized line defect, the heat did not have time to travel to the ends of the high

magnetic field region. This suggests that by measuring the origination of a second sound wave, the case of uniform heating can be distinguished from heating due to a defect. In the uniform heating case, OSTs will measure a second sound wave emanating from the nearest point on the high magnetic field region of the cavity, and will not all converge to a single point. In the defect case, the second sound wave must originate from a small region on the cavity surface, and the origin of these waves should converge to a line, or a point in the case of a highly localized defect.

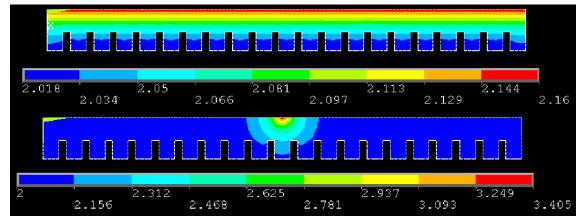


Figure 3: ANSYS simulation of heating of Niobium cavities initially at 2 K. Both the top and bottom surfaces dissipate the same power, but the bottom surface has its power dissipated in a defect 1/60th of the total area. Smaller defects lead to numerical instabilities for the transient solution.

METHODS

The experiments discussed here used a 1.3 GHz re-entrant design niobium cavity that was previously tested to have a maximum accelerating gradient of over 55 MV/m and made of Niobium with a RRR of 500 [1]. The cavity, LR1-3, was produced by Cornell University, and the cavity's history prior to this test is discussed elsewhere [5].

As discussed above, knowledge of the temperature of the RF surface is essential. To reduce the temperature increase of the RF surface during cavity operation, grooves 1.2 mm deep, spaced at 1 mm were machined on the cavity, and are shown in Fig. 4.



Figure 4: Photo of 1.3 GHz Niobium cavity with machined grooves to increase cooling. The grooves are 1.2 mm deep at 1 mm spacing.

After machining, the cavity was degreased, received a vertical EP removing \sim 5–10 μ m of material, degreased

again, was high pressure rinsed (HPR), and baked at 800°C for 2 hours. After the high temperature bake, the cavity received another 5–10 µm EP, ultrasonically cleaned and HPR. Finally the cavity was cleanly assembled, braced and pumped down, and then baked for 48 hours at 110 °C, a process which is known to reduce the high field Q-slope [7].

Previously, the cavity was driven with 200 µs pulses, but the latest experiment on this cavity used 150 µs of 1.5 MW HPP. Shorter pulses reduce energy dissipated in the cavity and ramp up cavity fields before any defects can heat the cavity and cause quench, so in general, the shorter the pulse length the better. The klystron power was coupled to the cavity such that the external quality factor could be adjusted between 10^5 and 10^6 . Coupling in this range balances quickly ramping up fields (taking about 100 µs) and being able to measure Q_0 accurately to determine when the normal conducting transition takes place.

Measuring the superheating field accurately relies on determining when the cavity transitions between the superconducting and normal conducting state. The transition time can be found by computing the quality factor of the cavity, a subject dealt with thoroughly in Hays' papers [3, 8]; here only the relevant equation is quoted. The intrinsic quality factor is related to the energy stored in the cavity according to

$$\frac{1}{Q_0} = \frac{2 \left(\sqrt{\frac{dP_f \omega}{dt}} - \frac{d\sqrt{U}}{dt} \right)}{\omega \sqrt{U}} - \frac{1}{Q_{ext}}. \quad (5)$$

where P_f , is the forward power, ω is the angular RF frequency, Q_{ext} is the “external” Q of the cavity, t is time, and U is the energy stored in the cavity.

Equation 5 can be used to calculate Q_0 as a function of time from measurements of P_f and U . When $Q_0 > 2 \times 10^6$, at least 90% of the cavity is superconducting [3]. Thus, solving $Q_0(t_{trans}) = 2 \times 10^6$, allows one to find the time when magnetic field at which the superconductor transitions into the normal conducting state. The value of the magnetic field at this time gives the superheating field: $H_{sh} = H(t_{trans})$. An example of a trace showing the magnetic field and Q_0 of the cavity as a function of time is shown in Fig. 5, illustrating how the superheating field is measured.

Eight OSTs were placed around the cavity. By measuring the arrival time of the second sound waves at different OSTs the quench location can be determined on the cavity [6]. As discussed, a local defect initiated quench can be distinguished from a global phase transition. Thus when all OSTs trigger simultaneously, the peak magnetic field gives the superheating field.

Finally, a Germanium resistive temperature detector was used to measure the bath temperature. This information both allows the inference of the speed of the second sound wave, and provides the initial temperature of the RF surface.

06 Material studies

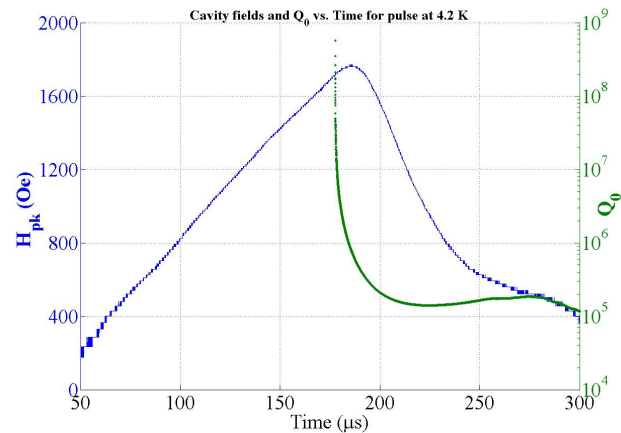


Figure 5: Plot of H_{pk} (blue line) vs time and Q_0 (green dots) vs time at 4.2 K for a pulsed measurement from the first cavity test. The RF power pulse lasted from 25–275 µs. The cavity becomes normal conducting at a peak field of 1760 Oe. Prior to this time, the Q_0 of the cavity is too high to be measured by methods used in pulsed operation.

MEASUREMENTS AND ANALYSIS

High pulsed power measurements were performed between 1.6 and 4.2 K and the results are plotted in Fig. 6. The Q versus E curve, taken at 1.6 K in CW operation is shown in Fig. 7. Though there was no field emission, note that there is high field Q-slope still present for this cavity

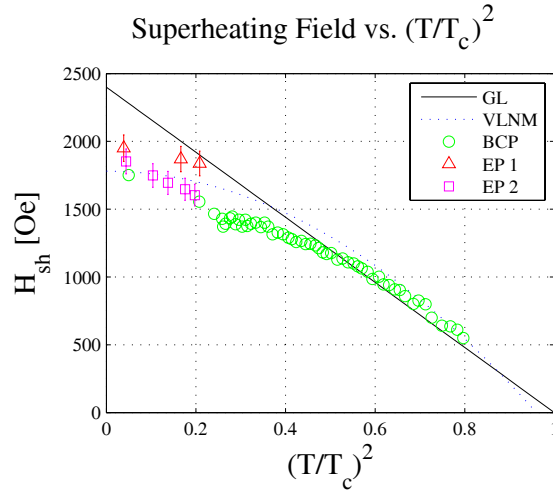


Figure 6: Graph of H_{sh} vs $(T/T_c)^2$, of experimental data and theory. The GL prediction is the solid line, and the VLNM is the dotted line. Circles mark selected points from Hay's BCP cavity test [8], the experiment with the ungrooved cavity is EP 1 and the grooved cavity is EP 2 on the plot. Field error bars of $\pm 5\%$ have been included corresponding to calibration uncertainty. Temperature errors are roughly the horizontal size of the markers.

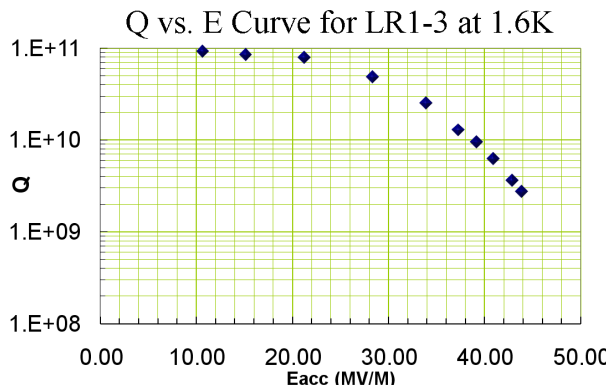


Figure 7: Q vs E curve for cavity LR1-3 in CW operation after machining grooves. The curve was taken at 1.6 K. The machining modified the cavity's resonant frequency from 1302 MHz to 1295 MHz.

even after a 110 °C bake.

Just as in the previous test with this cavity, no observed quenches were found to be due to localized cavity defects. The OST array measured second sound waves arriving simultaneously at all detectors, shown in Fig. 8. The second sound wave arrival times demonstrate that the detected waves emanate from areas on the high magnetic field region of the cavity nearest each detector. This region extends 1.5 cm on either side of the equator weld. The simultaneity of OST detections demonstrate that this entire region undergoes a phase change from the superconducting state to the normal conducting state. The phase change occurs in less than 5 μ s. All of this is consistent with observing a fundamental physical limit.

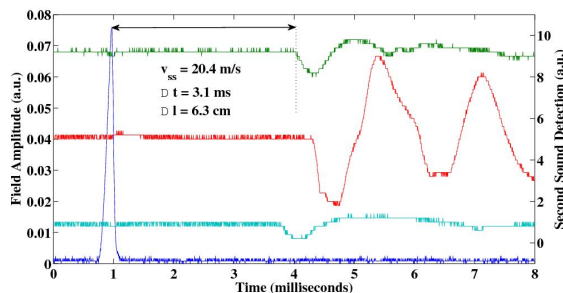


Figure 8: OST data for a single quench event. The lower trace is cavity field amplitudes, and the three upper traces are OST signals. The small time discrepancy between measured arrival times correspond to different OST positions. The OSTs all found the cavity quench to be a global event.

Previous measurements with Niobium cavities, processed with a buffered chemical polishing (BCP) process, were within 10% of the Ginzburg-Landau theory prediction down to a temperature of 6.2 K [3], but disagreed by 25% at 2 K. The VLNM, however, fits the single 2 K BCP data point to within 2%, but departs by 17.5% from measurement at the 4.2 K data point, while fitting high temperature data points as accurately as GL theory. Thus, the

06 Material studies

BCP results are insufficient to distinguish between the two theories, and further experimentation is necessary.

An experiment with the cavity was performed before machining cooling grooves [5]. These results cavity allows us to set a lower bound on the superheating field that agrees to within 3.5% of GL theory at a temperature of 4.2 K, but is 12% below the prediction at 2 K. The VLNM, however, under-estimates the 4.2 K point by 5% and the 2 K point by 13%.

The grooved cavity measurement of the superheating field coincide with the BCP cavity measurements at 4.2 K, but are 6% higher than the BCP cavity results at 1.6 K. This latest measurement is lower than the previous one. A possible explanation for this behaviour is that the field calibrations may be off by as much as 10%, from cell shape deformation due to cavity machining. This is supported by the fact that the resonant frequency of the cavity was 7 MHz lower than it was during the previous test. Preliminary simulations show that knowing the frequency shift is not enough to estimate the change in H_{pk}/E_{acc} , as this value is sensitive to exactly how the shape changes occurred.

Performing a linear fit to the latest data from Fig. 6 gave the fit line $H = -(1580 \pm 718)(T/T_c)^2 + (1917 \pm 105)$ Oe. A reasonable consistency check of the data is whether it passes through (1, 0), since at the critical temperature, one expects the superheating field to be zero. The x -intercept of this line is given by $x_0 = 1.21 \pm 0.55$. This intercept agrees with GL prediction, but the slope differs, suggesting that there are some systematic errors in the measurement. Origins of this error can arise from the magnetic field, electric field, or stored energy calibration or from the temperature measurement. Nevertheless, the results display a clear linear dependence on $(T/T_c)^2$, showing that the field increases with decreasing temperature down to 1.6 K. Though the latest data is not accurately described by Ginzburg-Landau Theory, which may in part be due to systematic effects just discussed, the superheating field shows a linear dependence $(T/T_c)^2$, and extrapolates to a zero H_{sh} at T_c , within error bars. All these features are shared with GL theory.

We now compare the VLNM with the experimental data. In the 1.6–4.2 K temperature range the VLNM is relatively flat. Linearising this model around 2.9 K, the middle of the temperature range, gives $H_{sh} \approx 1799 - 369 \left(\frac{T}{T_c}\right)^2$. While the y -intercept of this linearisation is 1σ less than the extrapolated value, the slope of this line is not consistent with the slope of the experimental data. These points, along with the fact that both tests measured fields > 1780 Oe, the maximum field allowed by VLNM, suggest that this model does not accurately model the superheating field of Niobium.

CONCLUSIONS

ANSYS simulations support the conclusion that uniform triggering of the OSTs are not caused by defects, but instead are a global phenomenon, supporting the claim that

the superheating field was indeed measured.

We were able to successfully determine the Q_0 of the cavity in pulsed mode, and use that information to determine the time of transition into the normal conducting state and thereby H_{sh} and the critical RF magnetic field. We demonstrated that the peak fields measured are fundamental limiting values because the entire high magnetic field region of the cavity changed from superconducting to normal conducting. The transition occurred in a span of a few microseconds, a time scale inconsistent with thermal break down or field emission. Furthermore, the OSTs show that the quench is not due to a local defect or field emission heating, adding further credence to the transitions occurring at a fundamental limit, the superheating field.

The VLNM predicts a saturation of the superheating field at 1780 Oe, a value surpassed in both tests. Also, the machined cavity results show H_{sh} increasing down to a temperature of 1.6 K. For this reason, it seems that GL theory, though not fully describing the superheating field, shares many features with our experimental data.

It should not be viewed as a deficiency in GL theory that the data does not exactly corroborate its predictions, because the theory is formulated to only be accurate near T_c , but it is still remarkable that the qualities this theory apply to data as far away as $T \sim 0.17T_c$.

REFERENCES

- [1] R. L. Geng et. al., "High Gradient Studies for ILC with Single-Cell Re-entrant Shape and Elliptical Shape Cavities Made of Fine-Grain and Large-Grain Niobium," *Proceedings of PAC07 WEPMS006* (2007).
- [2] H. Padamsee, J. Knobloch and T. Hays, "RF Superconductivity for Accelerators," (1998).
- [3] T. Hays, H. Padamsee and R. W. Röth, "Response of Superconducting Cavities to High Peak Power" in *Proceedings of the 1995 U.S. Particle Accelerator Conference*.
- [4] K. Saito, "Theoretical Critical Field in RF Application," Presented at *Pushing the Limits of RF Superconductivity Workshop* (2004).
- [5] N. Valles, et. al "Exploring the Maximum Superheating Magnetic Fields of Niobium," *PAC09, Vancouver, British Columbia, Canada, May 2009 TU5PFP052* (2009).
- [6] Z. A. Conway, et. al., "Defect Location in Superconducting Niobium Cavities Cooled with He-II Using Oscillating Superleak Transducers," *PAC09, Vancouver, British Columbia, Canada, May 2009 TU5PFP044* (2009).
- [7] G. Eremeev and H. Padamsee, "Change in High Field Q-Slope by Baking and Anodizing," *Physica C: Superconductivity* (2006).
- [8] T. Hays et. al., "Determining H_c^{RF} for Nb and Nb₃Sn through HPP and Transient Q Analysis," *7th Workshop on RF Superconductivity* (1995).
- [9] A. J. Dolgert et. al., "Superheating Fields of Superconductors: Asymptotic Analysis and Numerical Results," arXiv:cond-mat/9508085v1 21 Aug 1995.